RSC Advances

ROYAL SOCIETY OF CHEMISTRY

www.rsc.org/advances

Tetrathiafulvalene Derivatives as Cation Sensor: Density Functional Theory Investigation of the Hyper-Rayleigh Scattering First Hyperpolarizability

Chun-Guang Liu[1, 2*], Ming-Li Gao[1], Shuang Liu[1], Ding-Fan Zhang[1]

1 College of Chemical Engineering, Northeast Dianli University, Jilin 132012, Jilin Province, P. R. China;

2 Institute of Functional Material Chemistry, Faculty of Chemistry, Northeast Normal University, Changchun 130024, P. R. China

Abstract

The hyper-Rayleigh scattering (HRS) first hyperpolarizability of a series of extended (ex) tetrathiafulvalene (TTF) and TTF derivatives have been theoretically investigated using density functional theory (DFT) with the CAM-B3LYP functional to explore their use as potential cation sensor. Among these exTTF and TTF derivatives, a compound containing the redox-active TTF unit and chelating functional group pyridine is a an effective sensor for all five kinds of metal cation (Ni^{2+}, Cu^{2+}, Mg^{2+}, Zn^{2+}, and Cd^{2+}) studied here according to our DFT calculations. Compared with the

* Corresponding author.
Dr. Chun-Guang Liu
E-mail addresses: liucg407@163.com or liucg407@mail.nedu.edu.cn
Tel.: 86 0432 64806919. Fax: 86 0432 64806919.

traditional linear optical detection technology, the nonlinear optical property (HRS first hyperpolarizability) has rarely been considered to detect metal cation. Towards such goals, this compound would be useful to guide the search for potential cation sensor in new directions.

Keywords: tetrathiafulvalene; cation sensor; hyperpolarizability; nonlinear optical property; density functional theory

1. INTRODUCTION

The techniques of detecting metal ions have attracted considerable attention because of their potential application in chemistry, clinical biochemistry, toxicology, and environmental science, etc.[1-6] In general, the detection of metal ions is mainly based on the linear optical response. By contrast, the nonlinear optical (NLO) response has rarely been considered for detecting metal ions, especially second-order NLO property.[7] The advantages of second-order NLO response relevant to the linear optical response for detecting metal ions mainly come from the rich tensor component of the first hyperpolarizability.[8]

The interaction between a light wave and matter is frequently described through the induced electrical polarization ***P***. When a molecule is subjected to an external electric field F with high electric field strength, the molecular polarization ($\boldsymbol{p_i}$) can be written as

$$p_i = \sum_{\mathrm{j}} \alpha_{ij} F_j + \frac{1}{2} \sum_{j,k} \beta_{ijk} F_j F_k + \frac{1}{6} \sum_{j,k,l} \gamma_{ijkl} F_j F_k F_l + \cdots \qquad (1)$$

where α_{ij} is linear polarizability, β_{ijk} and γ_{ijkl} are the first hyperpolarizability and second hyperpolarizability, respectively. For the first hyperpolarizability, it is a third-rank (β_{ijk}) tensor, and has 27 components. These components are closely relative to the geometrical and electronic properties of molecules, and thus provide detailed and complicated detection fingerprints when compared with the linear optical responses. [9-10]

The molecular polarization $\boldsymbol{p_i}$ and the components of those tensors are functions of the frequency ω_1 induced by applied wave fields of frequency ω_2, ω_3, …ω_s in the

NLO processes. The frequency dependence of the polarization can be expressed as

$$p_i(\omega_1) = \sum_j \alpha_{ij}(-\omega_1;\omega_2)F_j(\omega_2) + \frac{1}{2}\sum_{j,k}\beta_{ijk}(-\omega_1;\omega_2,\omega_3)F_j(\omega_2)F_k(\omega_3) + \frac{1}{6}\sum_{j,k,l}\gamma_{ijkl}(-\omega_1;\omega_2,\omega_3,\omega_4)F_j(\omega_2)F_k(\omega_3)F_l(\omega_4)+\cdots \quad (2)$$

For the second-order NLO effect, four different kinds of phenomenon can be observed experimentally. They are second-harmonic generation [SHG; $\beta(-2\omega; \omega, \omega)$], the linear electro-optic effect [LEOE; $\beta(-\omega; \omega, 0)$], sum-frequency generation [SFG; $\beta(-\omega_1, -\omega_2; \omega_1, \omega_2)$], and optical rectification [OREC; $\beta(0; \omega, -\omega)$]. Among them, SHG has been used in chemical monitoring, biological and chemical sensing aspects.[11-13]

Hyper-Rayleigh scattering (HRS) is a widely-applied technology to measure SHG responses experimentally. Kim et al. demonstrated[14] that an appropriately functionalized gold nanoparticles was capable of sensing of ion contaminants in water via an ion-chelation-induced aggregation process based on their HRS studies. Their results clearly indicated that the HRS detection limit is much higher than that of linear optical spectroscopy. An enhancement of HRS responses was readily obtained with addition of as little as 25μM Pb^{2+}, this concentration too low to generate a visible color change. Darbha et al. reported[15] that the gold nanoparticles modified by mercaptopropionic acid and pyridinedicarboxylic acid can be used for screening of Hg(II) in aqueous solution with high detection limit (5 ppb) and selectivity over competing analyses. Their experimental results indicated that the HRS intensity is highly sensitive to the concentration of Hg(II) ions, the linear correlation was shown between the HRS intensity and the concentration of Hg(II) ions over the range of

5-100 ppb, which is the same order of magnitude as the environmental protection agency standard for the maximum allowable level of Hg(II) in drinking water.

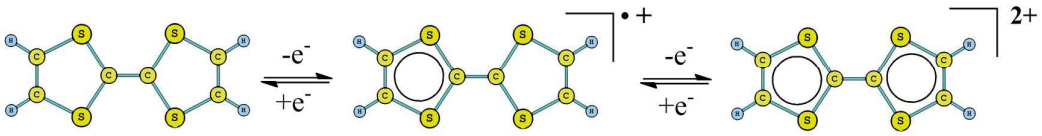

Chart 1. Continuous, reversible oxidation of TTF unit

The redox-active tetrathiafulvalene (TTF) unit[16] is able to exist in three different stable redox states (TTF, the radical cation $TTF^{\cdot+}$, and dication TTF^{2+}),[17] and the oxidation to the radical cation and dication occurs sequentially and reversibly at low potentials (see Chart 1). Due to the 14π-electron structure, the TTF unit is lack of a π-electrons cyclic conjugation, and thus is nonaromatic according to Hückel rule. But the radical cation and dication with one and two 6 π-electron units are aromatic in the Hückel sense, and thus both oxidized species are thermodynamically stable. Our previous studies found that the one-electron-oxidized process made the non-planar TTF units change to a planar structure, which improved its conjugation. And thus the oxidation leaded to a significant enhancement of the second-order NLO response.[18-25]

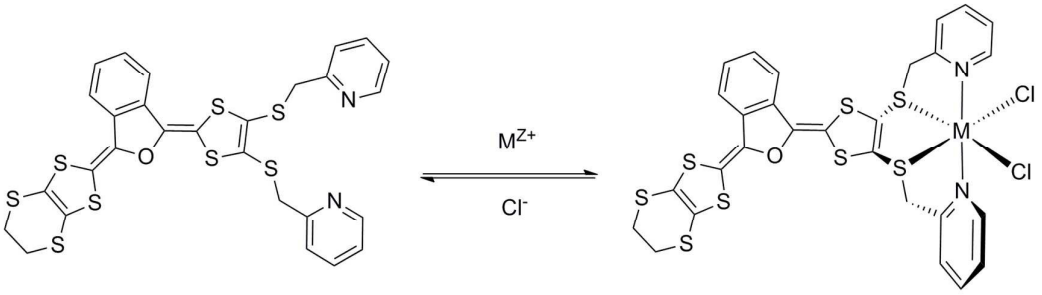

Chart 2. The structural formula of an exTTF derivative containing chelating pyridine functional groups

Recently, an extended (ex) TTF derivative, containing a furanoquinonoid spacer

and pyridine functional groups, has been prepared by Sallé group[26](see Chart 2). Because of the presence of pyridine with chelating functional groups, such exTTF derivatives can coordinate with various metal ions. According to the literature, introduction of metal ions into the organic molecules would generally increase the second-order NLO response.[27-47] This indicates that this kind of exTTF derivative may have a potential capability to detect metal ions.[48-51]

In the present paper, second-order NLO responses of a series of TTF derivatives containing the chelating pyridine functional group have been studied (see Fig. 1). The aim of this work is (i) exploration of the potential function for detecting metal ions on the basis of their hyper-Rayleigh scattering (HRS) response; (ii) analysis of the relationship between their redox properties and second-order NLO responses.

2. COMPUTATIONAL DETAILS

All molecular geometries were optimized and characterized as energy minima at B3LYP[52-54]/6-31G(d) levels (LANL2DZ basis set for metal atom). In order to obtain a more intuitive description of origin of the second-order NLO responses, time-dependent density functional theory (TDDFT) methods were used to describe the nature of excited state at CAM-B3LYP/6-31G(d) level (LANL2DZ basis set for metal atom).

The dynamic and static first hyperpolarizabilities have been calculated by using TDDFT method[55-56] with the long-range correction (LC) exchange-correlation functional in this work. HRS technology works equally well for neutral and charged species. In general, the dynamic first hyperpolarizability $\beta_{\mathrm{HRS}}(-2\omega;\omega,\omega)$ is analyzed in terms of its two contributions, originating from perpendicular light polarizations. Theoretically, Champagne et al.[57-58] have developed an effective method to estimate the molecular HRS response based on quantum chemical calculations, the molecular NLO response $\beta_{\mathrm{HRS}}(-2\omega;\omega,\omega)$ can be expressed as Bersohn theory:

$$\beta_{HRS}(-2\omega;\omega,\omega)=\sqrt{\left\{\left\langle\beta_{ZZZ}^{2}\right\rangle+\left\langle\beta_{XZZ}^{2}\right\rangle\right\}} \qquad (3)$$

Wherein, $\langle\beta^2_{ZZZ}\rangle$ and $\langle\beta^2_{XZZ}\rangle$ are orientational averages of the β tensor, which were calculated without assuming Kleiman's conditions.

For the DFT-derived hyperpolarizability, the conventional generalized gradient approximation and the localized density approximation always tend to overestimate hyperpolarizability of donor-π-conjugated bridge-acceptor (D-π-A) system,[59-60] even though the hybrid method such as B3LYP was used, the situation is not improved for

large D-π-A system. The deficiency of conventional exchange functional arises from the incorrect asymptotic exchange potential behavior, which results in an underestimation of charge–transfer excitation energies, and thus a large overestimation of hyperpolarizabilities. To overcome this problem, the LC exchange-correlation functional was developed. In the LC scheme, the DFT exchange and Hatree-Fock (HF) exchange contributions are partitioned at the operator level, and the proportion of nonlocal HF contribution varies in terms of the range of the interaction. The ratio of the nonlocal HF part to the local DFT part becomes larger for greater distances. And the interelectronic Coulomb operator is separated into a short-range component and its long-range complement. These improvement approaches offer a possibility to restore the correct asymptotic exchange potential behavior for the LC functionals. The literature reported that LC-DFT methods provide better estimates for hyperpolarizabilities in charge-transfer compound when compared with hybrid and GGA functionals.[61-65] Such as, the range-separated CAM-B3LYP functional with the proper consideration of the charge transfer between donor and acceptor well estimated molecular hyperpolarizability of D-π-A structure.

It is well known that the hyperpolarizability is sensitive to the electronic distribution in the fringe regions. Therefore, the basis set for calculating hyperpolarizability should involve both diffuse and polarized functions and be substantially larger than those required for calculating ground-state properties. For the metal atom, the SDD[66] basis set is more flexible because of its triplet–ζ quality when compared with the double–ζ quality LANL2DZ basis set. For the main group

elements, we explored basis set effects on the dynamic HRS first hyperpolarizability (β_{HRS}) using a variety of basis sets, including 6-31G(d), 6-31+G(d), 6-31++G(d), 6-311++G(d,p), and aug-cc-pVDZ for main groups. Due to the high computational cost, only the ligand **5** has been chosen as an example to consider the basis set effects in this work. The calculated β_{HRS} values of the ligand **5** with various basis sets have been listed in Table S1 (see Supporting Information). It can be found that the basis set effects on the β_{HRS} values are rather modest, introduction of diffuse function (6-31G(d) → 6-31+G(d)) only decreases the β_{HRS} value by 0.01×10^{-30} esu (-0.5 %). Further augmentation of the basis sets (6-31+G(d) → 6-31++G(d) and 6-31++G(d) → 6-311++G(d,p)) still produces the effects on the margins, increasing the β_{HRS} value by 0.16×10^{-30} esu (8%) and decreasing the β_{HRS} values by 0.1×10^{-30} esu (-5%), respectively. We compare the 6-311++G(d,p) and aug-cc-pVDZ data. The results indicate that the basis set effects remain marginal, the aug-cc-pVDZ β_{HRS} data is only 4% greater than the corresponding 6-311++G(d,p) value. Considering a balance between computational cost and accuracy, the 6-31+G(d) basis set may be an appropriate choice for our studied systems, and thus has been employed to calculate the dynamic HRS first hyperpolarizability of all compounds studied here. In the present paper, the dynamic first hyperpolarizability has been calculated at CAM-B3LYP[67]/6-31+g(d) levels (metal atoms using the SDD basis set). All calculations were performed using the Gaussian 09 program package.[68]

3. RESULTS AND DISCUSSION

3.1 Geometrical structure and second-order NLO properties

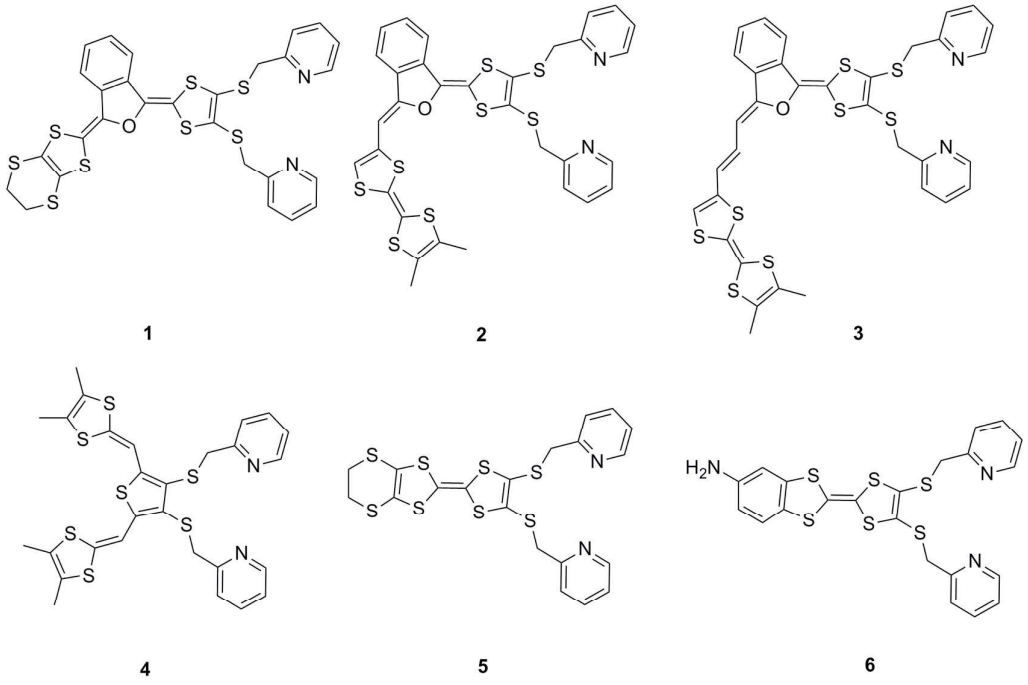

Fig. 1. The structural formula of the series of exTTF and TTF ligands

It has been reported that the ligand **1** can coordinate with various metal ions experimentally (see Chart 2). Moreover, the X-ray single crystal structure of an Ni(II) complex of the ligand **1** has been reported.[26] Since the ligand **1** is a quadridentate ligand, the octahedral coordination sphere of metal center need to be completed by two additional chloride ligands. In the present paper, the geometry of this Ni(II) complex has been optimized at B3LYP level using 6-31g(d) basis sets (LANL2DZ basis sets on metal atom). The key geometrical parameters of experimental and theoretical results have been compared in Table S2. It can be found that our DFT calculations well reproduce its geometrical structure. There is only a slight difference between calculated and experimental values, as comparison of the six bond lengths

around the metal center. The calculated average bond length is 2.373 Å, which is only 0.085 Å longer than the experimental value (2.288 Å). A comparison of the key bond and dihedral angles also shows good agreement between experimental and calculated parameters (see Table S2).

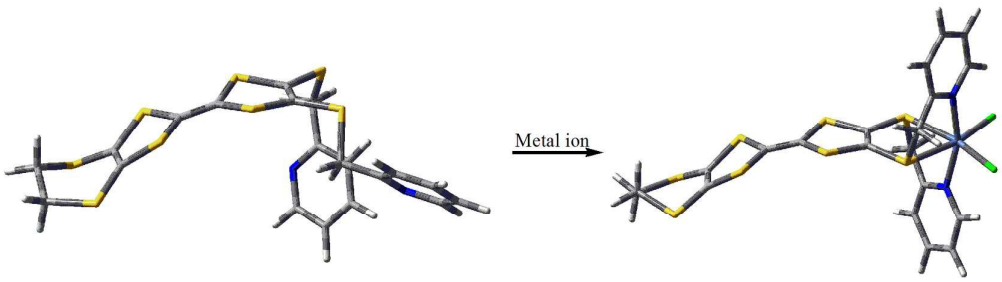

Fig. 2. Geometry structure of the ligand **5** and its metal complex

As an example, the molecular geometries of the ligand **5** and a metal complex optimized by our DFT calculations have been listed in Fig. 2. The optimized calculations offer a non-planar arrangement for the ligand **5**, where the TTF fragment is bent, and the two pyridine rings and the TTF unit are not on co-plane. Due to introduction of the metal ion, the conjugation of the metal complex gets an improvement when compared with the ligand **5**. As shown in Fig. 2, the metal center and the TTF unit can be viewed as co-planar roughly. This arrangement provides a favorable structural feature for enhancement of electronic interaction between TTF unit and metal center.

Table 1. HRS first hyperpolarizability (at 1064 nm in 10^{-30} esu) of the studied ligands and corresponding metal complexes and their one-electron-oxidized species obtained by CAM-B3LYP/6-31+g(d) calculations (SDD basis sets for metal atom)

Compounds	β_{HRS}	Compounds	β_{HRS}	Compounds	β_{HRS}	Compounds	β_{HRS}
Ligand **1**				Ligand **4**			
1	34.44	$\mathbf{[1]_{ox}}$	22636.15	**4**	53.21	$\mathbf{[4]_{ox}}$	2613.80
$\mathbf{Ni^{2+}}$	37.41	$\mathbf{[Ni^{2+}]_{ox}}$	22841.80	$\mathbf{Ni^{2+}}$	43.73	$\mathbf{[Ni^{2+}]_{ox}}$	2090.41
$\mathbf{Cu^{2+}}$	1507.40	$\mathbf{[Cu^{2+}]_{ox}}$	1376.70	$\mathbf{Cu^{2+}}$	997.31	$\mathbf{[Cu^{2+}]_{ox}}$	239000.00
$\mathbf{Cd^{2+}}$	48.27	$\mathbf{[Cd^{2+}]_{ox}}$	15048.41	$\mathbf{Cd^{2+}}$	30.49	$\mathbf{[Cd^{2+}]_{ox}}$	453.71
$\mathbf{Zn^{2+}}$	47.92	$\mathbf{[Zn^{2+}]_{ox}}$	1806.78	$\mathbf{Zn^{2+}}$	30.32	$\mathbf{[Zn^{2+}]_{ox}}$	426.00
$\mathbf{Mg^{2+}}$	37.04	$\mathbf{[Mg^{2+}]_{ox}}$	17243.70	$\mathbf{Mg^{2+}}$	28.65	$\mathbf{[Mg^{2+}]_{ox}}$	425.79
Ligand **2**				Ligand **5**			
2	65.16	$\mathbf{[2]_{ox}}$	468.00	**5**	1.99	$\mathbf{[5]_{ox}}$	289.13
$\mathbf{Ni^{2+}}$	83.38	$\mathbf{[Ni^{2+}]_{ox}}$	1031.24	$\mathbf{Ni^{2+}}$	3.68	$\mathbf{[Ni^{2+}]_{ox}}$	331.09
$\mathbf{Cu^{2+}}$	962.33	$\mathbf{[Cu^{2+}]_{ox}}$	549.58	$\mathbf{Cu^{2+}}$	3102.51	$\mathbf{[Cu^{2+}]_{ox}}$	1801.63
$\mathbf{Cd^{2+}}$	78.18	$\mathbf{[Cd^{2+}]_{ox}}$	641.93	$\mathbf{Cd^{2+}}$	18.75	$\mathbf{[Cd^{2+}]_{ox}}$	2939.55
$\mathbf{Zn^{2+}}$	76.53	$\mathbf{[Zn^{2+}]_{ox}}$	630.86	$\mathbf{Zn^{2+}}$	19.09	$\mathbf{[Zn^{2+}]_{ox}}$	2935.50
$\mathbf{Mg^{2+}}$	76.59	$\mathbf{[Mg^{2+}]_{ox}}$	681.25	$\mathbf{Mg^{2+}}$	26.52	$\mathbf{[Mg^{2+}]_{ox}}$	3188.20
Ligand **3**				Ligand **6**			
3	99.18	$\mathbf{[3]_{ox}}$	1808.54	**6**	3.77	$\mathbf{[6]_{ox}}$	2690.65
$\mathbf{Ni^{2+}}$	41.17	$\mathbf{[Ni^{2+}]_{ox}}$	1949.31	$\mathbf{Ni^{2+}}$	5.52	$\mathbf{[Ni^{2+}]_{ox}}$	1485.78
$\mathbf{Cu^{2+}}$	11884.8	$\mathbf{[Cu^{2+}]_{ox}}$	1413.30	$\mathbf{Cu^{2+}}$	24.17	$\mathbf{[Cu^{2+}]_{ox}}$	1584.08
$\mathbf{Cd^{2+}}$	38.19	$\mathbf{[Cd^{2+}]_{ox}}$	2229.33	$\mathbf{Cd^{2+}}$	2.42	$\mathbf{[Cd^{2+}]_{ox}}$	938.14
$\mathbf{Zn^{2+}}$	72.275	$\mathbf{[Zn^{2+}]_{ox}}$	2252.46	$\mathbf{Zn^{2+}}$	2.50	$\mathbf{[Zn^{2+}]_{ox}}$	879.69
$\mathbf{Mg^{2+}}$	39.74	$\mathbf{[Mg^{2+}]_{ox}}$	2153.49	$\mathbf{Mg^{2+}}$	2.93	$\mathbf{[Mg^{2+}]_{ox}}$	1117.75

In the present paper, five kinds of metal ions, Ni^{2+}, Cu^{2+}, Cd^{2+}, Mg^{2+} and Zn^{2+} have been considered as the target for detection. The dynamic first hyperpolarizability (β_{HRS}), which is closely associated with the HRS intensity, has been chosen as a source to analyze the detecting function of these exTTF and TTF derivatives. The β_{HRS} values of all compounds studied here have been calculated at CAM-B3LYP levels using 6-31+g(d) basis sets in this work (SDD basis sets for metal atom). The calculated β_{HRS} values have been listed in Table 1, and the HRS first

hyperpolarizability change of ligands and corresponding metal complexes has been compared in Fig. 3 and 4.

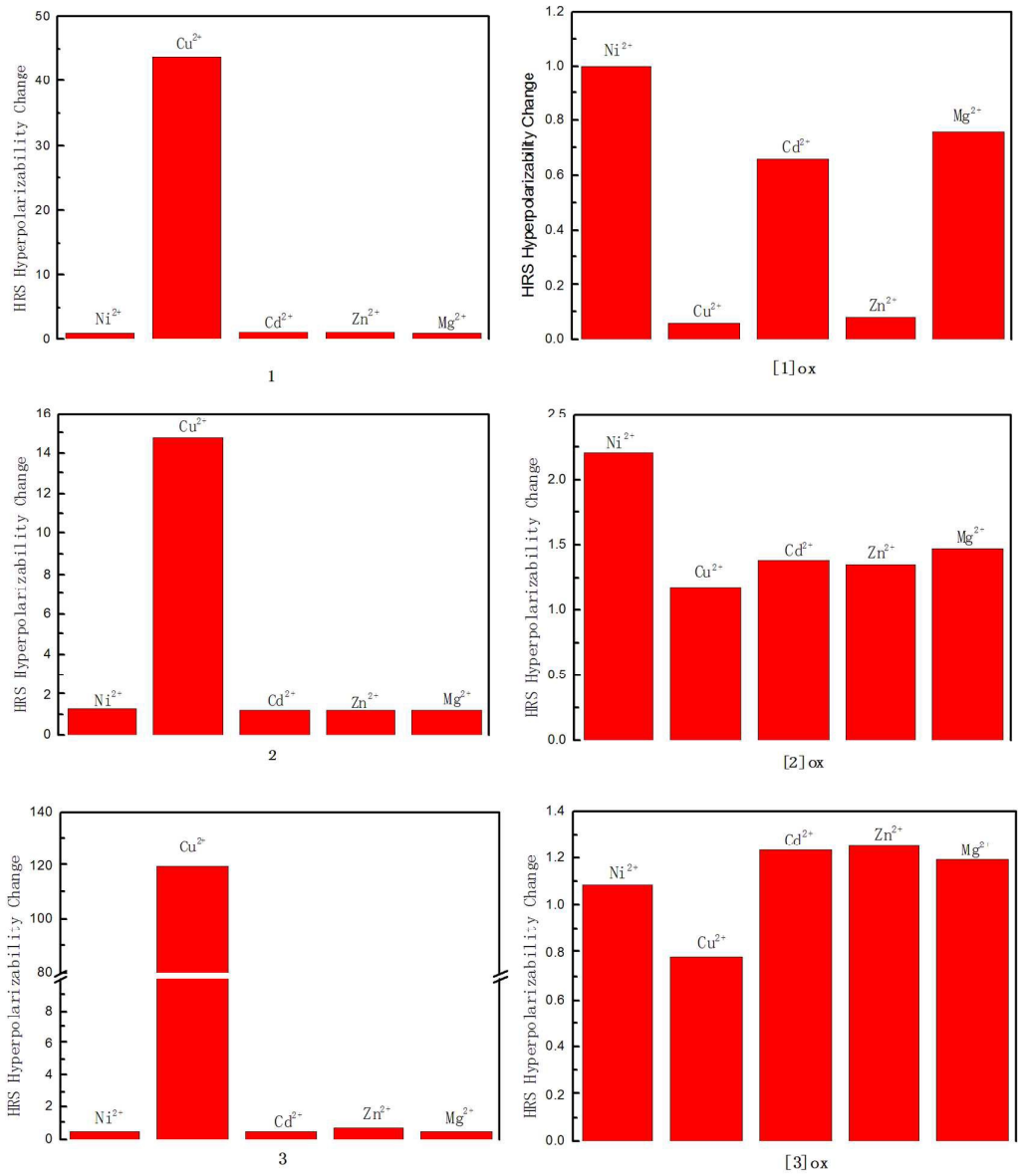

Fig. 3. Comparison of HRS first hyperpolarizability (at 1064 nm in 10^{-30} esu) change of ligands **1**-**3** and their corresponding metal complexes and that of one-electron-oxidized species obtained by CAM-B3LYP/6-31+g(d) calculations (SDD basis sets for metal atom)

For the ligand **1**, a substantial enhancement of the HRS first hyperpolarizability has been obtained when complexing Cu^{2+}, which leads to a 44-fold increase of the HRS first hyperpolarizability according to our DFT calculations (see Fig. 3). By contrast, the complexation of Ni^{2+}, Cd^{2+}, Mg^{2+} and Zn^{2+} do not largely affect the β_{HRS} value. The calculated β_{HRS} values of the one-electron-oxidized species of the ligand **1** and corresponding metal complexes also have been listed Table 1. It can be found that the β_{HRS} value of the ligand **1** gets a significant enhancement in the one-electron-oxidized process. The complexation of the five kinds of dication also modify the β_{HRS} value of the one-electron-oxidized species $\mathbf{[1]_{ox}}$. However, the β_{HRS} value of $\mathbf{[1]_{ox}}$ is not sensitive to introduction of Ni^{2+}, Cd^{2+}, and Mg^{2+}. By contrast, the complexation of Cu^{2+} and Zn^{2+} lead to a substantial decrease of the β_{HRS} value, respectively. The calculated β_{HRS} value of $\mathbf{[1]_{ox}}$ is about 10 times as large as that of corresponding Cu(II) and Zn(II) complexes, respectively. This indicates that $\mathbf{[1]_{ox}}$ has potential detecting function for Cu^{2+} or Zn^{2+}, but can not distinguish a mixture containing Cu^{2+} and Zn^{2+}.

In general, the first hyperpolarizability can be effectively tuned by lengthening the π-conjugated bridge in a suitable range. Thus, we have introduced the ethylene fragments into our studied system to design two new exTTF derivatives, ligands **2** and **3** (see Fig. 1). As shown in Table 1, the calculated β_{HRS} values in the order: **1 < 2 < 3**. Although the large HRS first hyperpolarizability would result in a strong signal, the detecting functional of ligands **2** and **3** can not be improve significantly when compared with the ligand **1**. For the ligand **2**, the complexation of Ni^{2+}, Cd^{2+}, Mg^{2+} and Zn^{2+} still do not largely affect the HRS first hyperpolarizability (see Fig. 3). And

the complexation of Cu^{2+} results in a 25-fold increase of the HRS first hyperpolarizability. After the one-electron oxidization, ligand **2** can not distinguish a mixture containing Cu^{2+}, Cd^{2+}, Mg^{2+} and Zn^{2+} because of the analogous magnitude of HRS first hyperpolarizability (β_{HRS}(C.)/β_{HRS}(L.) = 1.1-1.5), and the complexation of Ni^{2+} leads to a 2-fold increase of the HRS first hyperpolarizability. For the ligand **3**, the complexation of Ni^{2+}, Cd^{2+}, Mg^{2+} and Zn^{2+} lead to a decrease in HRS first hyperpolarizability, but the difference between them is not substantial (β_{HRS}(C.)/β_{HRS}(L.) = 0.4-0.7). And a 119-fold increase of the HRS first hyperpolarizability has been obtained when complexing Cu^{2+}. After the one-electron oxidization, ligand **3** almost loses its detecting function for all five kinds of dication studied here because of the analogous magnitude of the HRS first hyperpolarizability.

Heteroaromatic compounds have attracted considerable interest because of their large second-order NLO responses. Earlier studies[69-72] of heterocycle systems indicated that a decrease of the aromatic delocalization energy by the introduction of heterocycle would lead to the charge-transfer state dominated the ground state, and thus enhance the second-order NLO responses. Thus, we introduced the heteroaromatic fragment thiophene into our studied system to design another exTTF derivative, the ligand **4** (see Fig. 1). As expected, the HRS first hyperpolarizability of the ligand **4** is larger than that of the ligand **1** (see Table 1). The complexation of the Ni^{2+}, Cd^{2+}, Zn^{2+}, and Mg^{2+} all lead to a decrease of the HRS first hyperpolarizability for the ligand **4**. But the difference between them is not significant (β_{HRS}(C.)/β_{HRS}(L.) = 0.6-0.8). By contrast, the second-order NLO response gets a substantial

enhancement when complexing Cu^{2+}. The calculated β_{HRS} value of the Cu(II) complex is 19 times as large as that of the ligand **4**.

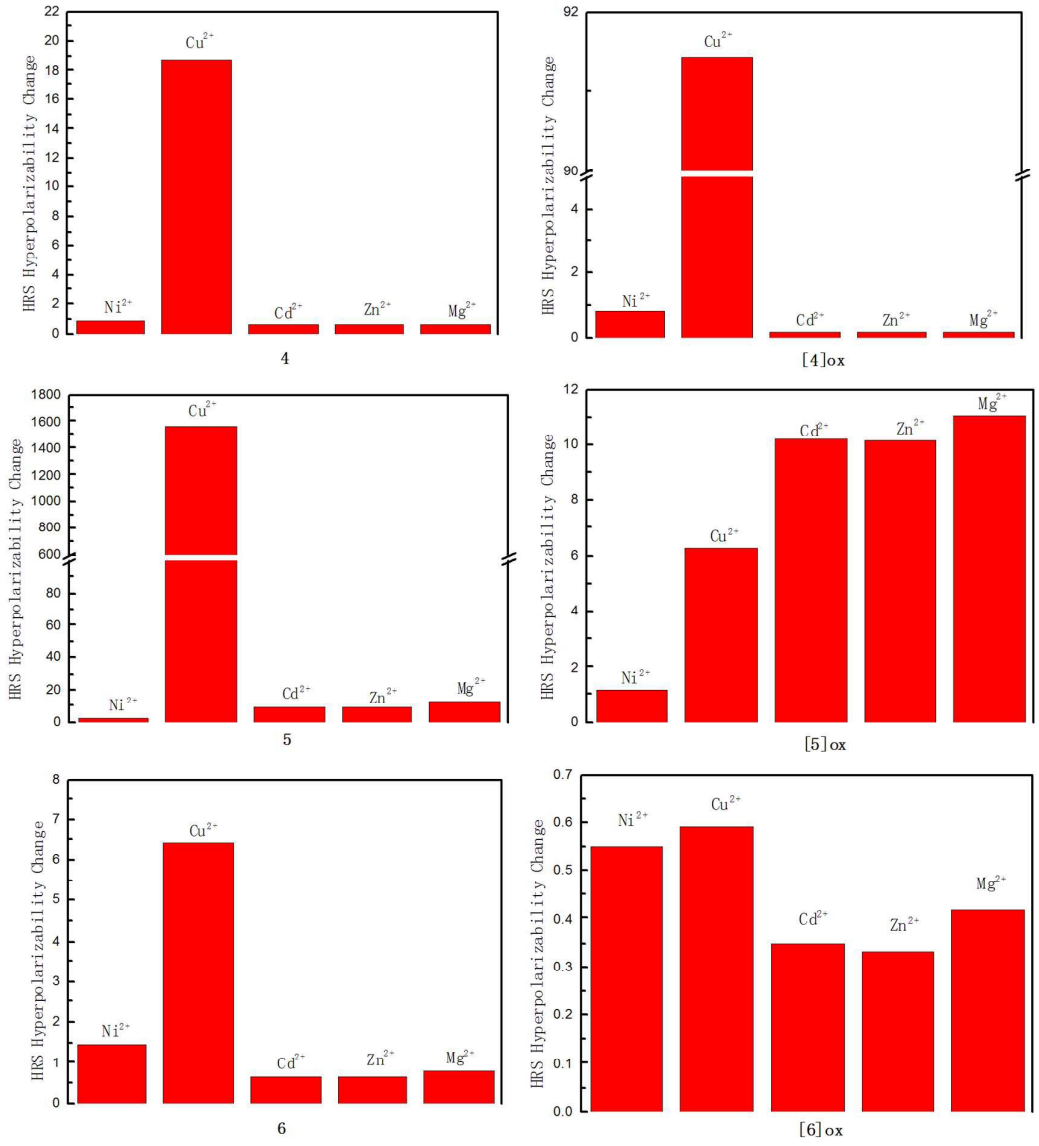

Fig. 4. Comparison of HRS first hyperpolarizability (at 1064 nm in 10^{-30} esu) change of ligands **4**-**6** and their corresponding metal complexes and that of one-electron-oxidized species obtained by CAM-B3LYP/6-31+g(d) calculations (SDD basis sets for metal atom)

The calculated β_{HRS} values of the one-electron-oxidized species of the ligand **4**

($[\mathbf{4}]_{ox}$) and corresponding metal complexes also have been compared in Fig. 4. It can be found that $[\mathbf{4}]_{ox}$ still has a large second-order NLO response when complexing Cu^{2+}. However, it is not possible to distinguish the Ni^{2+} owing to their analogous magnitude of HRS first hyperpolarizability (β_{HRS}(C.)/β_{HRS}(L.) = 0.8). The complexation of Cd^{2+}, Zn^{2+}, and Mg^{2+} still result in a decrease of the HRS first hyperpolarizability in a same range (β_{HRS}(C.)/β_{HRS}(L.) = 0.2), respectively. This indicates that $[\mathbf{4}]_{ox}$ has potential detecting function for Cd^{2+}, Zn^{2+}, and Mg^{2+} respectively, but can not distinguish a mixture containing Cd^{2+}, Zn^{2+}, and Mg^{2+}.

Due to the ligand **1** contains a furanoquinonoid spacer, the redox properties and second-order NLO responses would differ from the common TTF derivative. In the present paper, the exTTF unit has been replaced by the TTF unit to generate the ligand **5** (see Fig. 1). The calculated HRS first hyperpolarizabilities of the ligand **5** and corresponding complexes have been listed in Table 1. As expected, removal of the furanoquinonoid π-conjugated bridge leads to a decrease of the second-order NLO responses. Although the calculated β_{HRS} value of the ligand **5** is 17 times as small as that of the ligand **1**, the detecting function of the ligand **5** is prominent when compared with the ligand **1**. Our DFT calculations show that introduction of five kinds of dication all enhances second-order NLO response (see Fig. 4). The calculated β_{HRS} value is in the order $Cu^{2+} > Mg^{2+} > Zn^{2+} > Cd^{2+} > Ni^{2+}$. A strong signal should be a prerequisite for detecting metal ions. Towards such goals, the ligand **5** may be a good candidate for detection of all five kinds of metal ions. The complexation of Cu^{2+} leads to a 1560-fold increase of the HRS first hyperpolarizability. The complexation

of Mg^{2+} results in a 13-fold increase of the HRS first hyperpolarizability. The complexation of Cd^{2+} and Zn^{2+} lead to a 9-fold increase of the HRS first hyperpolarizability, respectively. And the complexation of Ni^{2+} results in a 2-fold increase of the HRS first hyperpolarizability. This indicates that the ligand **5** is an efficient sensor for every dications studied here, but it maybe lose its detecting capability for a mixture containing Cd^{2+} and Zn^{2+}.

The calculated β_{HRS} values of the one-electron-oxidized species of the ligand **5** and corresponding complexes also have been compared in Table 1 and Fig 4. It can be found that the β_{HRS} value of the ligand **5** gets a significant enhancement in the one-electron-oxidized process. The complexation of the five kinds of dication also increase the β_{HRS} value of the one-electron-oxidized species $\mathbf{[5]_{ox}}$. However, the variation in the HRS first hyperpolarizability (10-fold increase) is similar when complexing Cd^{2+}, Zn^{2+}, and Mg^{2+}. The complexation of Cu^{2+} gives rise to a 6-fold increase of the HRS first hyperpolarizability. And the complexation of Ni^{2+} does not largely affect the HRS first hyperpolarizability of $\mathbf{[5]_{ox}}$. This indicates that $\mathbf{[5]_{ox}}$ has potential detecting function for Cu^{2+}, Mg^{2+}, Zn^{2+}, and Cd^{2+}, but can not distinguish the Ni^{2+} and a mixture containing Cd^{2+}, Mg^{2+}, and Zn^{2+}.

It is well known that the typical organic NLO chromophore has mostly focused on the donor-π conjugated-acceptor (D-π-A) structure. According to our previous studies, the TTF unit never displays the character of electron donor because of the bent geometrical arrangement.[21,22] Thus we introduce an electron donor group (aniline group) into the ligand **5** to generate the ligand **6**. The calculated HRS first

hyperpolarizabilities of the ligand **6** and corresponding complexes have been compared in Table 1 and Fig. 4. Although the second-order NLO response of the ligand **6** gets a small enhancement with respect to the ligand **5**, the detecting function of the ligand **6** is unsatisfied. The largest variation appears when complexing Cu^{2+}, about 6 times as large as that of the ligand **6**. And the response of Ni^{2+} is not significant, a ~1.5-fold increase has been obtained according to our DFT calculations. The complexation of Cd^{2+}, $Mg^{2+}$and Zn^{2+} lead to the same variation of HRS first hyperpolarizability (β_{HRS}(C.)/β_{HRS}(L.) = 0.6-0.8), respectively. This indicates that it is hard to distinguish the Ni^{2+} and a mixture containing Cd^{2+}, Mg^{2+}, and Zn^{2+}.

The calculated β_{HRS} values of the series of one-electron-oxidized species of the ligand **6** also have been compared in Table 1 and Fig. 4. Although the β_{HRS} value of the ligand **6** gets a significant enhancement in the one-electron-oxidized process, the detecting function of $\mathbf{[6]_{ox}}$ is unsatisfied. A decrease of the β_{HRS} value of $\mathbf{[6]_{ox}}$ has been obtained when complexing all five kinds of metal dication, respectively. The complexation of Ni^{2+} and Cu^{2+} do not largely affect the HRS first hyperpolarizability (β_{HRS}(C.)/β_{HRS}(L.) = 0.6). And the complexation of Cd^{2+}, Mg^{2+} and Zn^{2+} still lead to a same variation of the HRS first hyperpolarizability (β_{HRS}(C.)/β_{HRS}(L.) = 0.4), respectively. All results indicate that the ligand **6** is not an efficient sensor for the five kinds of dication even though a one-electron oxidization has been carried out.

3.2. TDDFT studies

On the basis of the complex sum-over-states (SOS) expression, Oudar and Chemla

established a simple link between the molecular first hyperpolarizability and a low-lying energy charge transfer transition through the two-level model,[73, 74]

$$\beta_0 \propto \left(\mu_{ee} - \mu_{gg}\right)\frac{f_{os}}{\Delta E_{ge}^3}, \qquad (4)$$

where β_0 is the static first hyperpolarizability, μ_{gg} and μ_{ee} are the ground and excited state dipole moments, f_{os} is the oscillator strength, and ΔE_{ge} is the transition energy. Those factors (μ_{ee}-μ_{gg}, ΔE_{ge} and f_{os}) are all intimately related, and are controlled by electron properties of the donor/acceptor and the nature of the conjugated bridge. The optimal combination of these factors will provide the maximal β value.

Table 2. TDDFT result and static HRS first hyperpolarizability for the ligand **5** and corresponding metal complexes

Compounds	$\beta_{HRS}(0)$	Excited state	*E*(ev)	*λ*/*nm*	f_{os}	Major Contributions
5	1.27	6	4.67	265.3	0.472	HOMO→LUMO+6(47%) HOMO→LUMO+10(12%)
Ni^{2+}	1.79	22	4.16	298.1	0.104	*a*HOMO→*a*LUMO+6 (11%) *β*HOMO→*β*LUMO+8 (11%) *β*HOMO→*β*LUMO+11 (9%) *β*HOMO-5→*β*LUMO+2(8%)
Cu^{2+}	2.19	1	0.93	1340.3	0.003	*β*HOMO-2→*β*LUMO(+45%) *β*HOMO-29→*β*LUMO(+31%)
Cd^{2+}	1.30	7	4.71	263.2	0.317	HOMO→LUMO+7(+40%) HOMO→LUMO+1 (+15%)
Zn^{2+}	1.34	6	4.70	263.8	0.397	HOMO→LUMO+7 (+37%) HOMO→LUMO+1 (+28%)
Mg^{2+}	2.05	6	4.70	263.8	0.491	HOMO→LUMO+7 (46%) HOMO→LUMO+9 (13%)

In order to get more insights of changes in the HRS first hyperpolarizability of the various ligands when complexing metal ions, we have performed the TDDFT calculation on the excited state of all ligands and their metal complexes. The ligand **5**

and corresponding metal complexes have been chosen as examples to analyze the nature of the electronic transition. The TDDFT calculated excited energies, oscillator strengths, and associated orbital transitions of the ligand **5** and corresponding metal complexes have been listed in Table 2, and the rest of data has been listed in Table S3-S7 (see Supporting Information). For the ligand **5**, the TDDFT calculations show that the crucial excited state of the ligand **5** is the sixth excited state, which is formed by HOMO→LUMO+6 and HOMO→LUMO+10 transitions. The crucial excited state is defined as the lowest optically allowed excited state with substantial oscillator strength. These molecular orbitals associated with the crucial excited state have been listed in Fig. 5. It can be found that the HOMO of the ligand **5** mainly localizes on the TTF unit, and the LUMO+6 and LUMO+10 mainly delocalize over the TTF unit and one pyridine ring. Thus, these transitions would generate a weak charge transfer from the TTF unit to the pyridine ring.

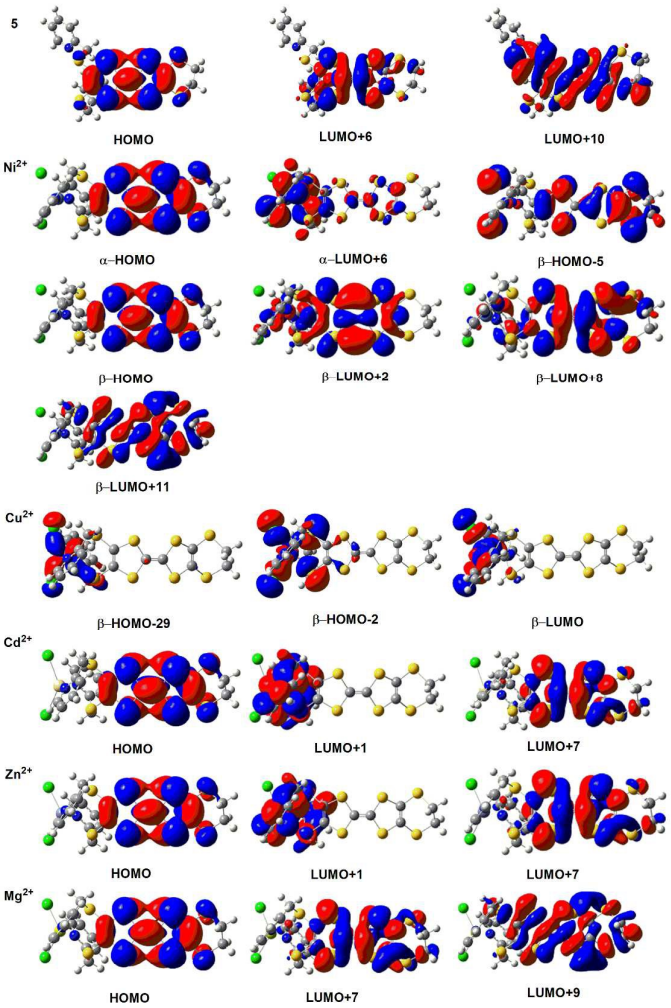

Fig. 5. The molecular orbital associated with the crucial excited states for the ligand **5** and its metal complexes

Our TDDFT calculations show that introduction of Ni^{2+}, Cd^{2+}, Zn^{2+}, and Mg^{2+} do not largely affect the magnitude of excited energy and oscillator strength. It is well-known that the static first hyperpolarizability is inversely proportional to the cube of excited energy and proportional to the oscillator strength, the analogous magnitudes of excited energy and oscillator strength imply small change of the static first hyperpolarizability when complexing Ni^{2+}, Cd^{2+}, Zn^{2+}, and Mg^{2+} cations. For the Cu(II) complex, a significant difference is obtained, where the calculated excited

energy and oscillator strength of the crucial excited state get a significantly decrease. The calculated excited energy decreases to 0.93 eV (1340 nm), which is about 5 times as small as that the ligand **5**. And the calculated oscillator strength decreases to 0.003 a.u., which is 157 times as small as that of the ligand **5** (We have checked the first ten excited state of the Cu(II) complex, the calculated oscillator strength is between 0.003 and 0.008. Although the oscillator strength of the first excited state is not largest among them, it has been chosen as the crucial excited state because of the very low-lying excited energy). Although the low-lying excited energy may lead to a large static first hyperpolarizability, the small oscillator strength would weaken this enhancement effect on the static first hyperpolarizability for the Cu(II) complex. In order to check the prediction by the TDDFT results, the static HRS first hyperpolarizability, $\beta_{HRS}(0)$, also has been calculated at CAM-B3LYP/6-31+g(d) level (SDD basis sets on metal atom) in this work. The calculated $\beta_{HRS}(0)$ values of the ligand **5** and corresponding metal complexes have been compared in Table 2. According to our DFT calculations, the magnitudes of the $\beta_{HRS}(0)$ for the ligand **5** and corresponding metal complexes are on the same order, ranging from 1.27 to 2.19 $\times$ 10^{-30} esu, which is well in agreement with our TDDFT predictions.

For the Cd(II) complex, the crucial excited state is formed by the HOMO→LUMO+7 and HOMO→LUMO+1 transitions. The molecular orbital associated with this crucial excited state has been listed in Fig. 5. It can be found that the HOMO still localizes on the TTF unit, and the LUMO+7 and LUMO+1 localize on the TTF unit, metal center, and pyridine ring. Thus these transitions would

generate a charge transfer from the TTF unit to the metal center and pyridine ring, and thus this excited state contains the ligand-to-metal charge-transfer (LMCT) transition. As shown in Table 2 and Fig. 5, the crucial excited state of the Zn(II) complex also displays the nature of LMCT transition. For the Ni(II) and Mg(II) complexes, there are no contributions from the metal center for these molecular orbitals. This indicates that these excited states arise from the intraligand charge transfer (ILCT) transitions. For the Cu(II) complex, the crucial excited state composes of βHOMO-2→βLUMO and βHOMO-29→βLUMO transitions. As clearly shown in Fig. 5, these molecular orbitals are metal-based d orbital of the Cu center. And thus it arises from the low-lying d-d transitions of metal center.

As shown in Fig. 4, the calculated dynamic HRS first hyperpolarizability of the Cu(II) complex for the ligand **5** is significantly larger than others. On the other hand, we have calculated the static HRS first hyperpolarizabilities of the Cu(II) complex (see Table 2). There is no significant enhancement of the $\beta_{HRS}(0)$ value when complexing Cu^{2+}. Thus, we believe that the large dynamic HRS first hyperpolarizability of the Cu(II) complex is mainly due to the frequency dispersion effects. The SOS expression for the dynamic first hyperpolarizability tensor is

$$\beta_{ijk}(\omega_\sigma;\omega_1,\omega_2)=\sum_p\sum_{m,n}\left\{\frac{\langle 0|i|m\rangle\langle m|\tilde{j}|n\rangle\langle n|k|0\rangle}{(E_{m,0}-\hbar\omega_\sigma)(E_{n,0}-\hbar\omega_2)}\right\} \qquad (5)$$

where i, j, and k are Cartesian coordinate indices. The operator $\tilde{j} = j$ - $\langle 0|j|0\rangle$, $E_{m,0}$ is the excited energy between the ground state and excited state m, $\langle 0|i|m\rangle$ is the transition dipole between the ground state and excited state m, $\langle m|i|n\rangle$ is the transition dipole between excited states m and n, ω_1 and ω_2 are incident photon frequencies, and

ω_σ is the output photon frequency. P permutes the pairs $\{i, -\omega_\sigma\}$, $\{j,\omega_1\}$, $\{k,\omega_2\}$. The sum over permutations produce six terms. When $\hbar\omega_\sigma$ or $\hbar\omega_2$ approaches $E_{m,0}$, the dynamic first hyperpolarizability tensor would increase significantly. In the present paper, an incident photon frequency at 1064 nm has been chosen to calculate the dynamic HRS first hyperpolarizability. As shown in Table 2, the excited energy of the Cu(II) complex is close to the incident photon frequency, which equals to 1340 nm. We also note that the excited energy of Cu(II) complexes in ligands **1**-**5** are almost constant ca. 0.9 eV (ca. 1300 nm) (see Supporting Information), which results to a significant enhancement of the HRS first hyperpolarizability when complexing Cu^{2+} for ligands **1**-**5**, which is well in agreement with our DFT calculations. As shown in Fig. 1, ligands **5** and **6** have analogous molecular structure. The calculated excited energy of the Cu(II) complex in the ligand **6** is 0.43 eV (ca. 2878 nm), which is lower than that of the ligand **5**. Although the Cu(II) complex in the ligand **6** possesses a low excited energy, the enhancement of the dynamic HRS first hyperpolarizability caused by the complexation of Cu^{2+} is not significant when compared with the ligand **5**. The dynamic HRS first hyperpolarizability of the Cu(II) complex is ~6 times as large as that of the ligand **6** (see Fig. 4). All results indicates that the magnitude of excited energy is a very important factor in determination of the dynamic HRS first hyperpolarizability. The excited energy closed to the incident photon frequency would lead to a significant enhancement of the dynamic HRS first hyperpolarizability because of the frequency dispersion effects.

4. CONCLUSIONS

In order to probe the potential detecting function for five kinds of metal ions (Ni^{2+}, Cu^{2+}, Mg^{2+}, Zn^{2+}, and Cd^{2+}) using their second-order NLO responses, the HRS first hyperpolarizabilities of a series of exTTF and TTF derivatives have been calculated at CAM-B3LYP/6-31+G(d) levels (SDD basis sets on metal atom). The result indicates that the detecting function of these exTTF and TTF derivatives can be tuned effectively. A compound containing the simple TTF unit and chelating functional group may be an efficient sensor for all five kinds of metal ions studied here. Meanwhile, the nature of excited state also has been analyzed on the basis of the TDDFT calculations. The results indicate that introduction of Ni^{2+}, Cd^{2+}, Zn^{2+}, and Mg^{2+} does not largely affect the magnitude of excited energy and oscillator strength. By contrast, complexation of Cu^{2+} leads to a significant decreases of excited energy and oscillator strength. Although the low-lying excited energy may lead to a large static first hyperpolarizability, the small oscillator strength would weaken this enhancement effect on the static first hyperpolarizability for the Cu(II) complex. The calculated static first hyperpolarizability of the ligand and its corresponding Cu(II) complex is on the same order. All results indicate that a significant enhancement of the dynamic HRS first hyperpolarizability in the Cu(II) complex is mainly due to the frequency dispersion effects.

Acknowledgments

The authors gratefully acknowledge the financial support from the National Natural

Science Foundation of China (21373043), Chinese Postdoctoral Science Foundation (2013M540261).

Supporting Information Available: The dynamic HRS first hyperpolarizability of the ligand **5** calculated by various basis sets, average bond length of the key bond and dihedral angles of experimental and the calculated parameters for an Ni(II) complex, the static HRS first hyperpolarizability ($\beta_{HRS}(0)$) and TDDFT result for the ligand **1-4,** and **6** and there corresponding metal complexes, and the optimized coordinates of the ligand **5** and its metal complexes. These materials are available free of charge via the Internet at http://pubs.rsc.org.

REFERENCES

1 C. Barranguet, M. Rutgers, A. M.Breure, M. Greijdanus, J. J. Sinke, W. Admiraal, *Environ. Toxicol. Chem.* 2003, **22***,* 1340 **-**1349.

2 L. K. Miao, X. F. Liu, Q. L. Fan, W. Huang, *Prog. Chem.* 2010, **22***,* 2338.

3 Q. Zhou, T. M. Swager, *J. Am. Chem. Soc*. 1995, **117**, 12593-12602.

4 M. R. Bryce, A. S. Batsanov, T. Finn, T. K. Hansen, A. J. Moore, J. A. K. Howard, *Eur. J. Org. Chem*. 2001, **5***,* 933-940.

5 J. D. Crowley, D. A. Leigh, P. J. Lusby, R. T. A. McBurney, *J. Am. Chem. Soc.* 2007*,* **129***,* 15085–15090.

6 X. H. Zhou, J. C. Yan, *J. Mater. Macromol.* 2004, **37**, 7078-7080.

7 M. R. Huang, Y. B. Ding, F. Y. Shi, X. G. Li, *Prog*. *Chem*. 2010, **24**, 2224-2233.

8 H. Stephan, C. Koen, P. Zoe, *Chem*. *Phys*. *Lett*. 1996, **258**, 485-489.

9 T. Verbiest, K.Clays, V. Rodriguez, *Nano. Lett*. 2009, **9**, 3945-3948.

10 P. Skabara, *Chem*. *Soc*. *Rev*. 2005, **34**, 69-98.

11 J. Becher, J. O. Jeppesen, K. Nielsen, *Synth. Met*. 2003, **309**, 133-134.

12 M. Sliwa, A. Spangenberg, I. Malfant, P. G. Lacroix, R. B. Pansu, K. Nakatani, *Chem*. *Mater*. 2008, **20**, 4062-4068.

13 J. L. Segura, N. Martín, *Angew*. *Chem*. *Int*. *Ed*. 2001, **40**, 1372-1409.

14 Y. Kim, R. C. Johnson, J. T. Hupp, *Nano Lett.* 2001, **1**, 165-167.

15 G. K. Darbha, A. K. Singh, U. S. Rai, E. Yu, H. Yu, P. C. Ray, *J. Am. Chem. Soc.* 2008, **130**, 8038-8043.

16 V. Barone, R. Improta, N. Rega, *Acc*. *Chem*. *Res*. 2008, **41**, 605-616.

17 D. Stefan, L. D. Franck, S. Marc, N. Antonia, D. Silvio, *Org*. *Lett*. 2007, **9**, 3753-3756.

18 B. Valeur, I. C. Leray, *Chem*. *Rev*. 2000, **205**, 3-40.

19 Y. L. Si, G. C. Yang, *J. Phys. Chem. A,* 2014, **118**, 1094–1102.

20 C. G. Liu, W. Guan, P. Song, L. K. Yan, Z. M. Su, *Inorg*. *Chem.* 2009, **48**, 6548-6554.

21 C. G. Liu, X. H. Guan, Z. M. Su, *J*. *Phys*. *Chem. C,* 2011, **115**, 6024–6032.

22 C. G. Liu, Z. M. Su, X. H. Guan, S. Muhammad, *J. Phys*. *Chem. C,* 2011, **115**, 23946–23954.

23 C. G. Liu, W. Guan, P. Song, Z. M. Su, C. Yao, *Inorg. Chem.* 2009, **48**, 8115–8119.

24 C. G. Liu, X. H. Guan, *Phys. Chem. Chem. Phys.* 2012, **14**, 5297–5306.

25 C. G. Liu, W. Guan, L. K. Yan, Z. M. Su, P. Song, *J. Phys. Chem. C,* 2009, **113**, 19672–19676.

26 D. Roberto, R. Ugo, *Organometallics*. 2000, **19**, 1775-1788.

27 J. L. Lyskawa, F. Le Derf, E. Levillain, M. Mazari, M. Sallé, *Eur. J. Org. Chem.* 2006, **10**, 2322-2328.

28 J. Lyskawa, M. Ocüafrain, G. Trippé, F. Le Derf, M. Sallé, P. Viel, S. Palacin, *Tetrahedron.* 2006, **62**, 4419-4425.

29 S. Silvi, A. Arduini, A. Pochini, A. Secchi, *J. Am. Chem. Soc*. 2007, **129**, 13378–13379.

30 D. R. Kanis, M. A. Ratner, T. Marks, *Chem. Rev.* 1994, **94**, 195-242.

31 A. Datta, S. S. Mallajosyula, S. K. Pati, *Acc. Chem. Res.* 2007, **40**, 213-221.

32 P. Innocenzi, B. Lebeau, *J. Mater. Chem.* 2005, **15**, 3821-3831.

33 M. M. Ayhan, A. Singh, C. Hirel, A. G. Gürek, V. Ahsen, E. Jenneau, I. Ledoux-Rak, J. Zyss, C. Andraud, Y. Bretonnière, *J. Am. Chem. Soc.* 2012, **134**, 3655−3658.

34 B. J. Coe, K. Clays, S. Foerier, T. Verbiest, I. Asselberghs, *J. Am. Chem. Soc*. 2008, **130**, 3286-3287.

35 A. Valore, E. Cariati, S. Righetto, D. Roberto, F. Tessore, R. Ugo, I. L. Fragalá, M. E. Fragalá, G. Malandrino, F. D. Angelis, L. Belpassi, I. Ledoux-Rad, K. H. Thi, J. Zyss, *J. Am. Chem. Soc.* 2010, **132**, 4966−4970.

36 H. M. Kima, B. R. Cho, *J. Mater. Chem.* 2009, **19**, 7402−7409.

37 B. J. Coe, J. L. Harries, M. Helliwell, L. A. Jones, I. Asselberghs, K. Clays, B. S. Brunschwig, J. A. Harris, J. Garin, J. Orduna, *J. Am. Chem. Soc.* 2006, **128**, 12192-12204.

38 S. Barlow, H. E. Bunting, C. Ringham, J. C. Green, G. U. Bublitz, S. G. Boxer, J. W. Perry, S. R. Marder, *J. Am. Chem. Soc*. 1999, **121**, 3715-3723.

39 M. Quintiliani, J. Pérez-Moreno, I. Asselberghs, P. Vázquez, K. Clays, T. Torres, *J. Phys. Chem. B,* 2010, **114***,* 6309–6315.

40 C. Dhenaut, I. Ledoux, I. D. W. Samuel, J. Zyss, M. Bourgault, H. Le Bozec, *Nature*. **1995**, *374,* 339–342.

41 C. Lee, W. T. Yang, R. G. Parr, *Phys. Rev*. 1988, **37**, 785-789.

45 M. Torrent-Succarat, M. Sola, M. Duran, J. M. Luis, B. Kirtman, *J. Chem. Phys.* 2004, **120**, 6346-6352.

43 I. D. L. Albert, J. O. Morley, D. Pugh, *J. Phys. Chem.* 1997, **101**, 1763-1766.

44 C. R. Moylan, S. Ermer, S. M. Lovejoy, I. H. McComb, D. S. Leung, R. Wortmann, P. Krdmer, R. J. Twieg, *J. Am. Chem. Soc.* 1996, **118**, 12950-12955.

45 P. Fischer, F. Hache, *Chirality.* 2005, **17**, 421-437

46 O. Maury, L. H. Bozec, *Acc. Chem. Res.* 2005, **38**, 691-704.

47 S. Keinan, M. J. Therien, D. N. Beratan, W. Yang, *J. Phys. Chem. A* 2008, **112**, 12203-12207.

48 B. Valeur, I. C. Leray, *Chem. Rev*. 2000, **205***,* 3-40.

49 G. K. Darbha, A. K. Singh, U. S. Rai, E. Yu, H. Yu, P. C. Ray, *J. Am. Chem. Soc.*

2008, *130*, 8038-8043.

50 Y. P. Zhao, L. Z. Wu, G. Si, Y. Liu, H. Xue, L. P. Zhang, C. H. Tung, *J. Org. Chem.* 2007, **72**, 3632-3639.

51 D. Stefan, X. L. Shi, L. D. Franck, N. Antonia, D. Silvio, *Org. Lett.* 2007, **9**, 3753-3756.

52 A. D. Becke, *Phys. Rev.* 1993, **98**, 5648-5652.

53 A. G. Baboul, L. A. Curtiss, P. C. Redfern, K. Raghavachari, *J. Chem. Phys.* 1999, **110***,* 7650-7657.

54 J. Tirado-Rives, W. L. Jorgensen, *J. Chem. Theory. Comput.* 2008, **4***,* 297-306.

55 E. Runge, E. K. U. Gross, *Phys. Rev. Lett.* 1984, **52**, 997−1000.

56 R. Bauernschmitt, R. Ahlrichs, *Chem. Phys. Lett.* 1996, **256**, 454−464.

57 B. Champagne, A. Plaquet, J. C. Pozzo, V. Rodriguez, F. Castet, *J. Am. Chem. Soc.* 2012, **134***,* 8101−8103.

58 B. Kirtman, B. Champagne, D. M. Bishop, *J. Am. Chem. Soc.* 2000, **122**, 8007-8012.

59 W. Kohn, A. D. Becke, R. G. Parr, *J. Chem. Phys*. 1996, **100***,* 12974-12980.

60 D. Qi, Y. Zhang, L. Zhang, J. Jiang, *J. Phys. Chem. A,* 2010, **114***,* 1931−1938.

61 D. Jacquemin, E. A. Perpète, G. E. Scuseria, I. Ciofini, C. Adamo, *J. Chem.Theory Comput.* 2008, **4**, 123−135.

62 E. A. Perpète, D. Jacquemin, C. Adamo, G. E. Scuseria, *Chem. Phys. Lett.* 2008, **456**, 101−104.

63 D. Jacquemin, E. A. Perpète, G. E Scuseria,. I. Ciofini, C. Adamo, *Chem. Phys.*

Lett. 2008, **465**, 226–229.

64 M. de Wergifosse, B. Champagne, *J. Chem. Phys.* 2011, **134**, 074113(1–13).

65 R. Zaleśny, I. W. Bulik, W. Bartkowiak, J. M. Luis, A. Avramopoulos, M. G. Papadopoulos, P. Krawczyk, *J. Chem. Phys.* 2010, **133**, 244308(1–7).

66 T. H. J. Dunning, P. J. Hay, Modern Theoretical Chemistry, *Ed. H. F. Schaefer III*. 1976, **3**, 1-28.

67 T. Yanai, D. Tew, N. Handy, *Chem. Phys. Lett.* 2004, **393**, 51-57.

68 M. J. Frisch, G. W. Trucks, H. B. Schlegel, G. E. Scuseria, M. A. Robb, J. R. Cheeseman, G. Scalmani, V. Barone, B. Mennucci, G. A. Petersson, H. Nakatsuji, M. Caricato, X. Li, H. P. Hratchian, A. F. Izmaylov, J. Bloino, G. Zheng, J. L. Sonnenberg, M. Hada, M. Ehara, K. Toyota, R. Fukuda, J. Hasegawa, M. Ishida, T. Nakajima, Y. Honda, O. Kitao, H. Nakai, T. Vreven, J. A. Montgomery, J. E. Peralta, F. Ogliaro, M. Bearpark, J. J. Heyd, E. Brothers, K. N. Kudin, V. N. Staroverov, R. Kobayashi, J. Normand, K. Raghavachari, A. Rendell, J. C. Burant, S. S. Iyengar, J. Tomasi, M. Cossi, N. Rega, J. M. Millam, M. Klene, J. E. Knox, J. B. Cross, V. Bakken, C. Adamo, J. Jaramillo, R. Gomperts, R. E. Stratmann, O. Yazyev, A. J. Austin, R. Cammi, C. Pomelli, J. W. Ochterski, R. L. Martin, K. Morokuma, V. G. Zakrzewski, G. A. Voth, P. Salvador, J. J. Dannenberg, S. Dapprich, A. D. Daniels, O. Farkas, J. B. Foresman, J. V. Ortiz, J. Cioslowski, D. J. Fox, Gaussian, Inc., Wallingford CT, 2009.

69 P. R. Varanasi, A. K.-Y. Jen, J. Chandrasekhar, I. N. N. Namboothiri, A. Rathna, *J. Am. Chem. Soc.* 1996, **118**, 12443-12448.

70 I. D. L. Albert, T. J. Marks, M. A. Ratner, *J. Am. Chem. Soc.*1997, 119, 6575-6582.

71 I. D. L. Albert, T. J. Marks, M. A. Ratner, *Chem. Mater.* 1998, **10**, 753-762.

72 E. M. Breitung, C. F. Shu, R. J. McMahon, *J. Am. Chem. Soc.* 2000, **122**, 1154-1160.

73 J. L. Oudar, D. S. Chemla, *J. Chem. Phys.* 1977, **66**, 2664–2668.

74 J. L. Oudar, *J. Chem. Phys.* 1977, **67**, 446–457.